Designing for Uniform Mobility Using Holonomicity

John Tighe Costa[1] and Mark Yim[2]

Abstract— **Holonomic systems are often complex and expensive with poor terrain handling capabilities. This paper introduces HAMR, a platform that is simple and low-cost with good terrain handling capabilities which was designed using a new method for characterizing mobility. A mobility ellipsoid (analogous to a manipulability ellipsoid) is introduced as a design tool. A metric called holonomicity measures the extent to which a vehicle can move equally in all directions. The holonomicity of HAMR is measured experimentally. It is shown that non-holonomic vehicles can have relatively high holonomicity as well.**

I. Introduction

There are many performance metrics for measuring a mobile robot's ability to traverse a workspace. Key metrics are typically top speed, maximum payload, cost and capacity for handling rough terrain. For some applications, however, the robot's ability to follow a specified arbitrary trajectory is also critical. This trajectory following ability is a function of the robot's kinematic design.

Holonomic mobile bases are those without constraints on their direction of motion. Automobiles are not holonomic because they cannot instantaneously move sideways (thus the need for parallel parking). Holonomic mobile bases have been studied for several decades and have a wide variety of uses where mobile agility is critical. Potential applications include mobile manipulation [1], pursuit, or movie camera tracking.

There are a variety of common misconceptions with holonomic drives.

- Drive mechanisms with zero turning radius are sometimes misclassified as holonomic. To follow a trajectory with sharp corners, these vehicles must stop to reorient their wheels; holonomic vehicles can change directions without stopping. Two non-holonomic, zero turning radius vehicles are the differential drive Pioneer P3-DX [2] and synchro-drive Real World Interface B12 [3].
- While vehicles with fewer controllable degrees of freedom (DOF) than total workspace DOF (three in the case of land-based mobile robots) must be non-holonomic, having equal or more controllable than total DOF does not guarantee holonomy.

Past holonomic approaches include specialized wheels such as unidirectional frictional wheels, typically with rollers or wheels mounted around the circumference, omni-wheels [4], Swedish wheels or Mecanum wheels [5], orthogonal wheels [6], and ball wheels [7].

[1]John Tighe Costa is a Master's student of Robotics, Univ. of Pennsylvania, Philadelphia, PA 19104, USA tighe.costa@gmail.com

[2]Mark Yim in the Dept. of Mech. Eng. and Applied Mechanics, Univ. of Pennsylvania, Philadelphia, PA 19104, USA yim@seas.upenn.edu

Rollers-on-rim wheel systems suffer from poor terrain handling: obstacle navigation is limited by the roller radius, not the wheel radius. Many sizable robots that use these rollers-on-rim wheels cannot drive over relatively small bumps such as power cords and carpet thresholds. Since each roller needs its own bearing surface, these wheel systems are also mechanically complex and costly. The other cited holonomic drive examples require more actuators than the minimum (3) to achieve holonomy so are expensive, complicated, and heavy.

Differential drives are a common, low cost, non-holonomic drive system that can be designed to have zero turning radius. We reintroduce the modification of adding an offset turret to a differential drive base to achieve holonomy [8], and we apply a novel optimization criteria to choose geometric parameters. This mechanism uses the minimum number of actuators and simple wheels, enabling lower cost and complexity than the cited alternatives without sacrificing terrain handling.

II. Mobility Ellipse as a Performance Metric

There is a duality between locomotion and manipulation. Whereas a robot manipulator moves its end effector relative to its base, the robot locomotor moves its base relative to the ground. The locomotor can be considered to be manipulating the world.

Yoshikawa [9] characterizes the response of a manipulator arm responds to a unit input by deriving an equation based on the Jacobian that describes an ellipsoid, the *manipulability ellipsoid*. We will introduce an extension of this tool for characterizing mobility.

The Jacobian maps joint-space velocities to end-effector velocities in the workspace for a given set of joint positions. We can derive the velocities, force, or torque required at the joints to attain a specified end-effector reaction. The manipulability ellipsoid visualizes achievable relative velocities, rather than absolute velocities; its utility is its ability to examine workspace dimensions relative to each other.

We extend the concept manipulability ellipsoid to wheeled mobile robots (WMRs) and call it the *mobility ellipsoid*, (ME). After choosing a drive mechanism, we use the mobility ellipsoid to optimize the geometric parameters.

The ME of an WMR is a visual representation of the robot's achievable medial (forward/backward), lateral (sideways) and rotational velocities, where the Cartesian axes of the plot correspond to the body DOF. For clarity, we include the ME's projection into the $\dot{Y}\dot{X}$ plane, its "shadow," in the following figures.

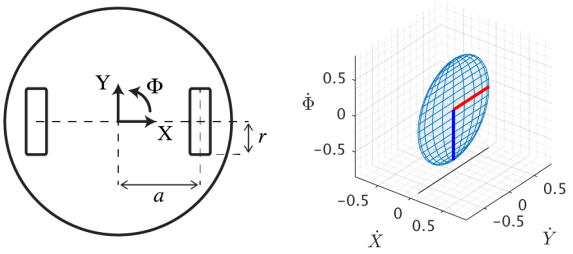

Fig. 1. a) DDR configuration b) Isometric image of ME for DDR $r = a = 1$

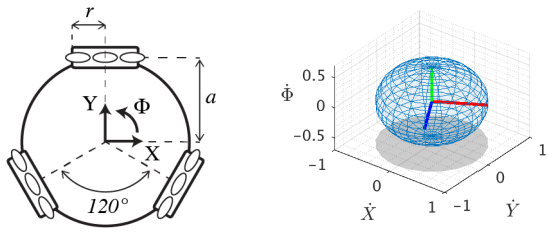

Fig. 3. a) ODWMR schematic b) Isometric image of ME for ODWMR $r = a = 1$

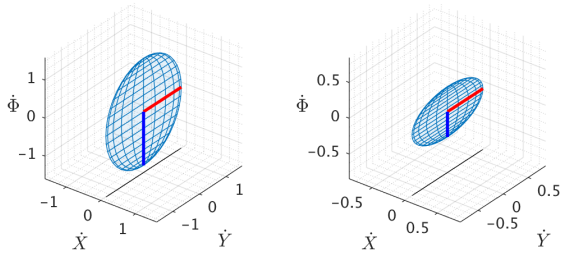

Fig. 2. a) Isometric image of ME for DDR $r = 2, a = 1$, b) $r = 1, a = 2$

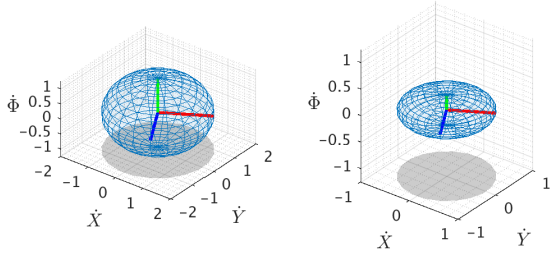

Fig. 4. a) Isometric image of ME for ODWMR $r = 2, a = 1$ b) $r = 1, a = 2$

For example, the ME for a differential drive robot (DDR) is pictured in Figure 1b. As indicated by the ellipsoid's shadow, a DDR cannot translate laterally ($\dot{X} = 0$) and the ME is contained in $\dot{Y}\dot{\Phi}$ plane. The shape of the ellipsoid reflects the relationship between a DDR's achievable translational and rotational velocities: $\dot{Y}_{max} = 0 | \dot{\Phi} = \dot{\Phi}_{max}$, and $\dot{\Phi}_{max} = 0 | \dot{Y} = \dot{Y}_{max}$.

Increasing the radius of a DDR's drive wheels by a factor of two scales the ellipse, as the new robot would be able to move at twice the previously achievable speeds (Figure 2a). Increasing a DDR's wheel separation by a factor of two compresses the ellipse, as the new robot would be able to translate just as quickly as before but rotate at half of the previous speed (Figure 2b).

As a second example, the ME for a 3-wheeled omnidirectional WMR (ODWMR) is pictured in Figure 3b. Since ODWMR's are holonomic, the ME is three-dimensional. As indicated by the circular shadow, an ODWMR's maximum rate of translation is the same in any direction. Cross sections containing the $\dot{\Phi}$ axis are oval, as the robot's achievable rotational and translational velocities are inversely related (as in the case of the differential drive robot).

As with a DDR, increasing wheel radius by a factor of two scales the ellipsoid by two (Figure 4a). Increasing the distance from each wheel to the center of the robot vertically compresses the ellipse, as the new ODWMR's translational mobility is unaffected, while its rotational mobility is reduced (Figure 4b).

Note that we assume a unit velocity vector, i.e. that there is a joint actuator maximum velocity limit (e.g. independent of payload, inertias etc.) when considering the envelope of the ellipsoid.

III. Holonomicity

Rather than adhering to the classical mobility binary of holonomic or non-holonomic, we can use the mobility ellipsoid to compare WMRs on a continuum. We introduce the concept of *holonomicity* as the extent to which a vehicle can move equally in all global DOF.

For WMRs, which have two translational and one rotational DOF, equal mobility in all DOF would seem to imply that robots with spherical ME have more holonomicity than those without. As seen in the case of the ODWMR, a ME with a circular $\dot{X}\dot{Y}$ projection indicates equal lateral and medial mobility, an intuitive conclusion given that both motions have the same units. However, metric differences between translation and rotation complicate the interpretation of the $\dot{X}\dot{\Phi}$ and $\dot{Y}\dot{\Phi}$ projections. The characteristic of these projections from which we draw significant conclusions is symmetry; MEs that are symmetric about the $\dot{\Phi}$ axis represent vehicles whose rotational mobility depends only on the speed of translation, not the direction. We observe that a WMR for which the ME is symmetric about the $\dot{\Phi}$ axis has higher holonomicity than one for which the ME is asymmetric.

We use projections and intersections of a WMR's ME to guide geometric parameter selection. Projections of the ME into a normal plane of motion show the relationship between mobility in those two DOF in that plane irrespective of mobility in the third. The projection into the $\dot{X}\dot{Y}$ plane shows the envelope of possible translational velocities. For a DDR, this projection reveals that DDRs cannot translate laterally, but does not show the inverse relationship between achievable translational and rotational speeds.

Cross-sections of the ME illustrate the relationship between between mobility in two DOF, given a constant velocity in the third. For example, the intersection of a ME with the $\dot{X}\dot{Y}$ plane ($\dot{\Phi} = 0$) shows a WMR's capacity for translating without rotating; the intersection with the plane $\dot{Y} = \dot{Y}_{max}/2$ shows a WMR's ability to translate laterally and rotate when translating forward at half its max speed.

The desired shape of the ME depends on the application. For a warehouse robot that stocks shelves or an assembly line robot that transports then installs components, it may be that the robot's orientation matters only at the beginning and end of its motion, while path following and speed are most important during transit. For a camera robot that films a target or a vehicle in tight pursuit, it may be that rotational mobility is important all the time. When using the ME as a design tool, it is useful to look at both projections and intersections. The projection of the ME into the $\dot{X}\dot{Y}$ plane shows the mobility relevant during transit. The intersection of the ME with that plane reflects the mobility relevant at the beginning and end of transit. The cost of design decisions such as whether or not to change actuators or geometry can then be evaluated with respect to the improvement in application-specific performance. It may be worth altering the $\dot{X}\dot{Y}$ intersection for a service or camera robot which regularly operates in orientation-constant conditions, but not for a warehouse or assembly line robot.

IV. Differential Drives with an Offset Turret

Differential drives can be made holonomic if a turret is added whose axis is not situated between the drive wheels. The RAMSIS II mechanism analyzed by El-Shenawy et al. in [8] presents such a configuration. Synchro-drives can similarly be made holonomic by adding a turret and choosing a non-central reference point (e.g. the front point) [10]. These configurations are simple and efficient holonomic drive mechanisms.

We classify the RAMSIS II [8] architecture as a differential drive with offset turret (DDROT) mechanism, pictured in Figure 5. It consists of two layers. The lower layer is a conventional differential drive base, and the upper layer is a turret that rotates about an axis offset from the rotational center of the lower layer.

This configuration can be understood as analogous to a swivel caster. The mounting plate of a swivel caster (gray, Figure 6a) can be considered as having three passive DOF: wheel rotation (red axis), wheel heading (green axis), and turret rotation (blue axis). Other holonomic drive systems use multiple actuated swivel casters [1].

The DDROT is the actuated equivalent of a single swivel caster. The two DOF of the differential drive lower layer correspond to the wheel rotation and wheel heading of the swivel caster (red and green axes, respectively), though the wheel heading is not directly controlled by the swivel caster alone, and the single DOF of the offset turret corresponds to the turret rotation of the swivel caster (blue axis). Actuation of these three DOF results in holonomic control of the turret (gray, Figure 5b) and whatever is mounted to it.

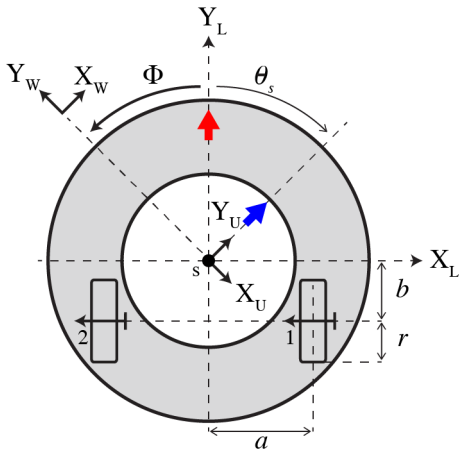

Fig. 5. Diagram of example configuration with DOF

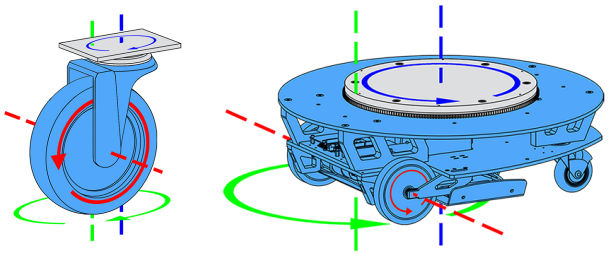

Fig. 6. DOF of a) swivel caster and b) DDROT

The DDROT drive mechanism is characterized by three parameters, as seen in Figure 5: wheel radius r, wheel separation $2a$, and turret offset b. Designers are often tempted to set $b = 0$, especially if the plan form profile is circular, so the drive wheels can have the largest possible separation and the system has some symmetrical elegance. However, holonomic motion is only possible when $b > 0$, as will be shown in Section V.

V. Effects of Drive Mechanism Geometry

El-Shenawy et al. introduces the DDROT architecture, but provides no guidelines for the design parameters of the mechanism; we use the ME method presented in Section II as a design tool to direct the selection of geometric parameters for the DDROT. The forward Jacobian transforming actuator velocities $\dot{q}_s = [\dot{\theta}_{x1}, \dot{\theta}_{x2}, \dot{\theta}_s]$ to global velocities $\dot{p}_s = [\dot{X}, \dot{Y}, \dot{\Phi}]$ for the system shown in Figure 5 is

$$J = \begin{bmatrix} -r(bc+as)/(2a) & r(bc-as)/(2a) & 0 \\ -r(bs-ac)/(2a) & r(bs+ac)/(2a) & 0 \\ r/(2a) & -r/(2a) & -1 \end{bmatrix} \quad (1)$$

[8] where s and c are $\cos(\theta_s)$ and $\sin(\theta_s)$ respectively. The ME for the DDROT mechanism with $r = a = b = 1$ is shown in Figure 7a. Projections of the ME generated from Eqn. 1 into the $\dot{X}\dot{Y}$, $\dot{X}\dot{\Phi}$ and $\dot{Y}\dot{\Phi}$ planes, with the intersection of the ellipsoid with that plane highlighted, are presented in Figures 7b, 8a and 8b.

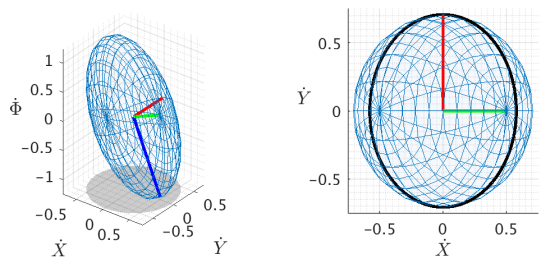

Fig. 7. a) Isometric view of ME for RAMSIS II: $r = a = b = 1$ b) Projection into $\dot{X}\dot{Y}$ plane, intersection with $\dot{X}\dot{Y}$ plane highlighted

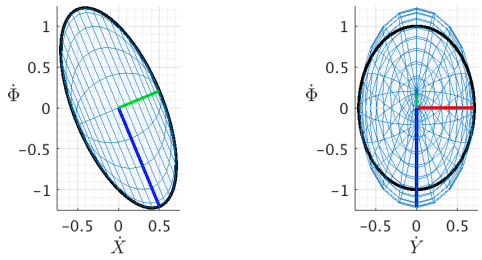

Fig. 8. a) Projection of ME for DDROT ($r = a = b = 1$) into $\dot{X}\dot{\Phi}$ plane, $\dot{X}\dot{\Phi}$ intersection with plane highlighted b) Projection into $\dot{Y}\dot{\Phi}$ plane, intersection with plane highlighted

A. Pure Translational Mobility

The projection of the mobility ellipse into the $\dot{X}\dot{Y}$ plane (Figure 7b, blue mesh) is circular when $a = b$, indicating that the medial ($\dot{Y}$) and lateral ($\dot{X}$) velocities are uniform. Considering only the differential drive lower layer of DDROT, one can intuit this relationship by observing that the robot's origin and the wheels are equidistant from the lower layer's center of rotation when $a = b$.

A more interesting relationship is presented in the intersection of the ME with the $\dot{X}\dot{Y}$ plane (Figure 7b, black line), corresponding to mobility while maintaining ($\dot{\Phi} = 0$). Here, the robot can translate medially ($\dot{Y}$) faster than it can translate laterally ($\dot{X}$). Lateral translation necessitates rotation of the differential drive; the turret must rotate at the opposite rate to maintain heading. The rate of pure lateral translation is thus constrained not only by the geometry of the differential drive lower layer, but also by the rate at which the turret can rotate.

B. Orientation Bias

The mobility ellipse for the DDROT is not symmetric. The projection of the ellipsoid into (and intersection with) the $\dot{X}\dot{\Phi}$ plane is skewed (Figure 8a). It follows from the previous discussion of the effects of turret speed on orientation-constant lateral motion that there is a relationship between lateral and rotational mobility. As compared to moving in the $\pm Y$ (aligned with wheel, where no lower layer rotation occurs), moving the $\pm X$ direction results in lower layer rotation directly proportional with the translation speed. This rotational velocity is then added to any turret rotation, thus linearly coupling the X direction velocity with rotational velocity. The skew angle reflects this coupling. We call this asymmetry "orientation bias," and it is most apparent in the outer shape of the ellipsoid - operation at the maximum velocities. For example, the robot can rotate counter-clockwise more quickly when translating in the $-X$ direction than when translating in the $+X$ direction.

C. Design Solutions

To improve robot holonomicity, we need to make the ellipsoid more uniform. We present three possibilities.

First, we can increase turret offset b relative to wheel separation a, increasing the robot's lateral mobility. The further the turret is offset from the center of rotation of the differential drive, the greater the ratio of lateral to rotational velocity; this is the same as increasing r in the equation for circular motion, $v_{tan} = \omega \cdot r$. The ME for $b = 2a$ is presented in Figures 9a and 9b. This approach is useful during the early stages of WMR design, when drive geometry can be altered.

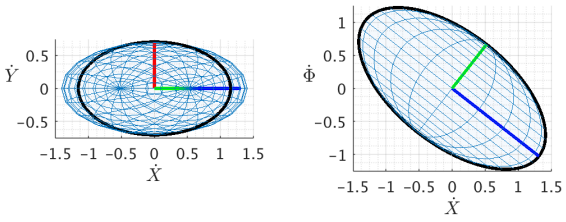

Fig. 9. a) Projection of ME for DDROT ($r = 1, a = 1, b = 2$) into $\dot{X}\dot{\Phi}$ plane, intersection with plane highlighted b) Projection of ME for DDROT ($r = 1, a = 1, b = 2$) into $\dot{Y}\dot{\Phi}$ plane, intersection with plane highlighted

Second, we can decrease the wheel radius r relative to turret offset b and wheel separation a. Reducing wheel size lowers the maximum speed of the differential drive. The ME for $r = a/2 = b/2$ is presented in Figures 10a and 10b. It should be noted that changing wheel size will effect the robot's terrain handling.

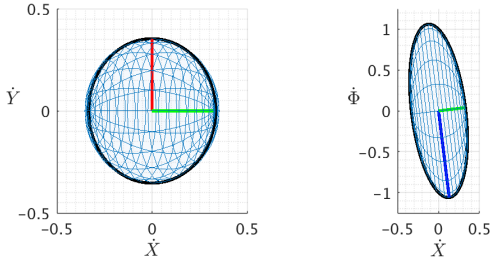

Fig. 10. a) Projection of ME for DDROT ($r = 0.5, a = 1, b = 1$) into $\dot{X}\dot{Y}$ plane, intersection with plane highlighted b) Projection into $\dot{X}\dot{\Phi}$ plane, intersection with plane highlighted

Third, we can adjust the speed of the turret relative to the drive wheels. As explained previously, the maximum orientation-constant lateral velocity is, constrained by the

capacity of the turret to counter-rotate against the differential drive lower layer in the nominal case. Turrets that rotate faster relative to their differential drive base enable the robot to maintain orientation through faster lateral movements. The ME for a configuration where the turret can rotate as quickly as the differential drive base is presented in Figures 11a and 11b. Note that the intersection line in Figure 11a is nearly circular. This solution can be applied to retrofit existing robots if different motors of similar form factor can be swapped in.

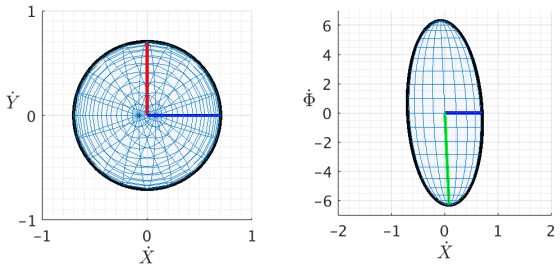

Fig. 11. a) Projection of ME for DDROT ($J(3,3) = -2\pi, r = a = b = 1$) into $\dot{X}\dot{Y}$ plane, intersection with plane highlighted b) Projection into $\dot{X}\dot{\Phi}$ plane, intersection with plane highlighted

VI. HAMR Implementation

HAMR stands for Holonomic Affordable Multi-terrain Robot and is pictured in Figure 12.

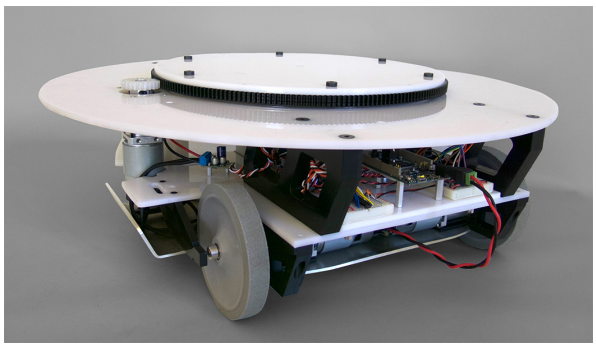

Fig. 12. HAMR, a DDROT optimized using the ME.

The HAMR vehicle's drive mechanism is an example of a DDROT whose geometric parameters were optimized using the ME. The project goal was to build a low-cost robotic platform capable of traversing typical indoor terrain with maximum holonomicity. The indoor terrain is classified as that compliant with the 2010 ADA Standards for Accessible Design [11] which includes obstacles such as floor bumps up to $1.27cm$.

HAMR's chassis is concentric with the turret's axis of rotation in order to maintain a circular footprint through its motion. We chose an outer diameter of $60cm$ for functionality as a mounting platform and maneuverability through ADA compliant space. We chose $r = 6.15cm$ wheels to meet the terrain handling requirements. We found the maximum elevator-car to floor gap ($3.175cm$[11]) to be primarily responsible for driving wheel size. The turret is compatible with a family of gearboxes so HAMR's holonomicity can be adjusted post-production without chassis modification.

The design results, summarized in Table I, show HAMR's ability to handle all ADA compliant indoor terrain.

Metric	Target	HAMR
Translational Speed	1.0 m/s	1.23 m/s
Rotational Speed	180 $^\circ/s$	270 $^\circ/s$
Incline Ratio*	1:12	1:6
Level Change*	1.27 cm	1.78 cm
Threshold Height*	1.91 cm	1.91 cm
Floor Gap*	3.17 cm	3.81 cm
Payload	20 kg	30 kg
BOM Cost	$1000	$967.75

*from ADA accessibility regulations [11]

TABLE I
Summary of HAMR Implementation Performance

We used the ME to choose the turret offset b and wheel separation $2a$. It proved impossible to achieve symmetric constant-heading translational mobility (a circular $\dot{X}\dot{Y}$ cross section) while maintaining a $60cm$ robot diameter. By holding $a = b$, however, we established equal orientation-variable translational motion (a circular shadow). We minimized the skew angle by increasing a and b as much as possible within the diameter constraint, yielding $a = b = 16.41cm$.

HAMR's ME is pictured in Figure 13a, 13b and 14, respectively.

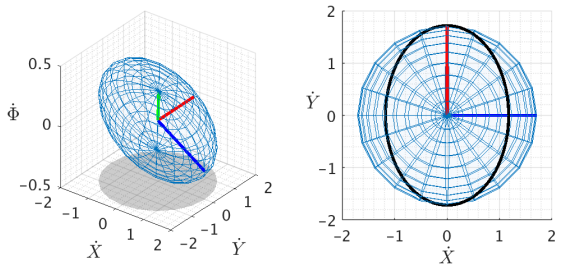

Fig. 13. a) isometric image of ME for HAMR b) Projection of ME for HAMR II into $\dot{X}\dot{Y}$ plane, intersection with plane highlighted

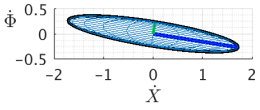

Fig. 14. Projection of ME for HAMR II into $\dot{X}\dot{\Phi}$ plane, intersection with plane highlighted

VII. Discussion

The holonomicity as defined in Section III applies to instantaneous changes in velocity for analyzing theoretically ideal cases; we now introduce an empirical measure for mobility we call *measured holonomicity*.

Given a starting configuration S that fully defines the robot state in the workspace and a target configuration T that is

a fixed distance d_T from the current position, and rotated θ_T from the current orientation, the robot is commanded to move from a stopped state at S to stopped at T in the fastest manner possible while measuring the time t to complete.

We can find a measured holonomicity for a given θ_T, $H(\theta)$ by measuring the travel time to reach all positions $T(d_T)$ at a fixed distance d_T from the robot origin

$$H(\theta) = \frac{t_{min}}{t_{max}} \tag{2}$$

where t_{min} is the time of the shortest path of all $T(d_T)$ and t_{max} is the longest. Note that the minimum direction and maximum direction are often known prior to experimentation, so typically only two measurements are needed. For example, a car will have t_{min} when it moves straight, t_{max} will occur when parallel parking. The overall holonomicity H is the worst case (smallest) $H(\theta)$ for all θ.

The t_{min} values serve to normalize the H values. So in the best case, the maximum holonomicity, $H = 1.0$, indicates uniform mobility capability, i.e. motions in all directions are the same. The worst case, $H = 0$, occurs if there exists a θ in which motions could not be achieved ($t_{max} = \infty$).

This definition also allows comparison of non-holonomic systems. For example, car-like non-holonomic vehicles can translate sideways, but more slowly than most DDRs, and thus H would be smaller.

Note that the choice of d_T will affect the measured values of H. In fact as d_T approaches 0, the measured H approaches the theoretical, $\hat{H}$, which describes instantaneous velocity capabilities for a given pose. We can thus find $\hat{H}$ from ME which is defined as

$$\hat{H}(\theta) = \frac{\hat{t}_{min}}{\hat{t}_{max}} \tag{3}$$

where $\hat{t}_{min}$ and $\hat{t}_{max}$ are minimum and maximum distance from the center to the surface of the ME and can be determined from the eigenvalues of the Jacobian. Note that for non-holonomic vehicles $\hat{H} = 0$.

For HAMR, $H = 0.81$. The t_{min} was measured moving straight forward 1m with wheels aligned and $\theta = 0$. The t_{max} trajectory was moving straight 1m laterally starting with the differential drive initially oriented forwards. As can be seen in Figure 13b the translations are not uniform. In hindsight, the third design technique mentioned in Section V-C of increasing the turret speed would yield a higher H for this test.

The Willow Garage PR2 has four powered casters whose caster turning axles are not offset, thus the system is non-holonomic. The same 1m trajectories to measure H for HAMR resulted in $H = 0.74$. The fast caster rotation yields this relatively high value. For many applications, this difference would be unnoticed; indeed it is a common misconception that the PR2 system is holonomic.

VIII. Conclusion

In this paper, we propose a novel metric, *holonomicity*, for measuring the ability of a wheeled mobile robot to follow a specified arbitrary trajectory. We also presented an extension of the manipulability ellipsoid to apply to mobility. This extension, which we call the mobility ellipse, provides a design tool for optimizing the geometric parameters of a given WMR configuration. We used the mobility ellipse to design a low cost platform called HAMR. Not only does HAMR have high holonomicity, but it also has better terrain crossing capabilities than more complicated wheel holonomic configurations such as omni-wheel bases. While we use the mobility ellipse exclusively as a tool for selecting specific geometric parameters, we believe that it has potential as a powerful performance metric to compare different WMR configurations.

Acknowledgements

The authors would like to acknowledge Andrew Specian and Daniel Edgar for their help in testing HAMR; Golam Kibria, John Kim and Christian Wang for their help creating HAMR; Melonee Wise for pointing us to RAMSIS II; Braden McDorman for PR2 measurements; and the support of NSF grant CNS-1513108.

References

[1] R. Holmberg and O. Khatib, "Development and control of a holonomic mobile robot for mobile manipulation tasks," *The International Journal of Robotics Research*, vol. 19, no. 11, pp. 1066–1074, 2000.

[2] MobileRobots, "Omron adept: Pioneer p3-dx," http://www.mobilerobots.com/ResearchRobots/PioneerP3DX.aspx, September 2016.

[3] P. Caloud, W. Choi, J.-C. Latombe, C. Le Pape, and M. Yim, "Indoor automation with many mobile robots," in *Intelligent Robots and Systems' 90.'Towards a New Frontier of Applications', Proceedings. IROS'90. IEEE International Workshop on*. IEEE, 1990, pp. 67–72.

[4] H. Asama, M. Sato, L. Bogoni, H. Kaetsu, A. Mitsumoto, and I. Endo, "Development of an omni-directional mobile robot with 3 dof decoupling drive mechanism," in *Robotics and Automation, 1995. Proceedings., 1995 IEEE International Conference on*, vol. 2. IEEE, 1995, pp. 1925–1930.

[5] O. Diegel, A. Badve, G. Bright, J. Potgieter, and S. Tlale, "Improved mecanum wheel design for omni-directional robots," in *Proc. 2002 Australasian Conference on Robotics and Automation, Auckland*, 2002, pp. 117–121.

[6] F. G. Pin and S. M. Killough, "A new family of omnidirectional and holonomic wheeled platforms for mobile robots," *IEEE transactions on robotics and automation*, vol. 10, no. 4, pp. 480–489, 1994.

[7] M. West and H. Asada, "Design and control of ball wheel omnidirectional vehicles," in *Robotics and Automation, 1995. Proceedings., 1995 IEEE International Conference on*, vol. 2. IEEE, 1995, pp. 1931–1938.

[8] A. El-Shenawy, A. Wellenreuther, A. S. Baumgart, and E. Badreddin, "Comparing different holonomic mobile robots," in *2007 IEEE International Conference on Systems, Man and Cybernetics*. IEEE, 2007, pp. 1584–1589.

[9] T. Yoshikawa, "Manipulability of robotic mechanisms," *The international journal of Robotics Research*, vol. 4, no. 2, pp. 3–9, 1985.

[10] S. Temizer and L. P. Kaelbling, "Holonomic planar motion from non-holonomic driving mechanisms: The front-point method." in *Intelligent Systems and Advanced Manufacturing. International Society for Optics and Photonics*, 2002.

[11] U. D. of Justice, "2010 ada standards for accessible design," www.ada.gov/regs2010/2010ADAStandards/2010ADAStandards.pdf, September 2010.